Journal of Sound and Vibration (1998) **216**(2), 199–213
Article No. sv971666

A COMBINED TUNED ABSORBER AND PENDULUM IMPACT DAMPER UNDER RANDOM EXCITATION

F. S. COLLETTE

Department of Structural Engineering and Materials, Technical University of Denmark, DK-2800 Lyngby, Denmark

(*Received* 20 *October* 1997)

Vibration control capability of a combined tuned absorber and impact damper, under a random excitation, is investigated numerically and experimentally. The effectiveness of the optimal combined absorber and its sensitivity to variations of the clearance, restitution coefficient and the mass ratio between the impact damper and tuned absorber are analyzed. The performance of the combined absorber is compared to the corresponding optimal conventional tuned absorber with viscous damping, with special emphasis on sensitivity to tuning and damping of the tuned absorber.

1. INTRODUCTION

A tuned vibration absorber is a classical passive controller of excessive vibrations around the resonant frequencies of lightly damped structures [1]. The tuned absorber is simply a single-degree-of-freedom mechanical oscillator attached to the primary structure and tuned to the frequency to be controlled. This results in significant attenuation of the vibration amplitudes of the primary system at the tuning frequency. However, the combined primary and absorber system has now two resonance frequencies, one on either side of the considered resonance frequency of the primary system. The frequency response of this two-degree-of-freedom system would not pose a practical problem, if it could be ensured that the frequency of excitation is virtually constant at the tuning frequency. This expectation is unrealistic, when considering random vibrations of civil engineering structures, which are induced mainly by wind-load and seismic action. Hence, a supplementary technique to attenuate vibrations at both resonances is necessary to ensure the reliability of the tuned absorber.

An effective reduction of the excessive oscillations at these two resonance frequencies can be obtained by introducing adequate viscous damping in the conventional tuned absorber. This corresponds to the well-known Tuned Mass Damper (TMD) [1–3]. The TMD is successfully used in several civil engineering structures, such as towers and bridges, in which viscous damping of the TMD is introduced by different hydraulic mechanisms. These mechanisms can be rather complicated and demand continual maintenance to ensure presence of the desired damping. A comparatively cheap and maintenance free system to enhance the performance to a tuned absorber is the impact damper.

An impact damper [4–6] is basically a lumped mass colliding intermittently with the structure to be controlled. The impact damper considered here is a small rigid ball placed in a container attached to a resonant primary structure. A small clearance is left between

0022–460X/98/370199 + 15 $30.00/0

the container and the impact damper. Impacts may occur as soon as the displacement of the primary system exceeds the clearance. Every collision produces some energy dissipation and some exchange of momentum between the colliding bodies. Energy dissipation is sometimes helpful in attenuating the excessive vibration amplitudes of the primary structure, but the important control mechanism is the exchange of momentum during collisions. For an adequate choice of clearance, the primary structure and impact damper move in opposite directions before collision. The direction of motion of the smaller impact damper is reversed after a collision, whereas the velocity of the primary structure is only reduced due to its larger inertia. As a result of the reduced velocity, the primary system attains a smaller displacement amplitude than it would have without impacts. Here, the impact damper is therefore introduced into the tuned absorber to control its oscillations and thereby indirectly reduce the excessive vibrations of the primary structure [7, 8]. The optimal effectiveness and the sensitivity to parameter variations of this combined tuned absorber and impact damper is investigated.

2. THE EXPERIMENTAL MODEL

2.1. THE PRIMARY STRUCTURE

The plane three-floor steel frame presented in the picture and sketch of Figure 1 was available and therefore chosen as the primary structure to be controlled. Such a frame structure could represent a flexible tower-like building. The test frame is composed of steel

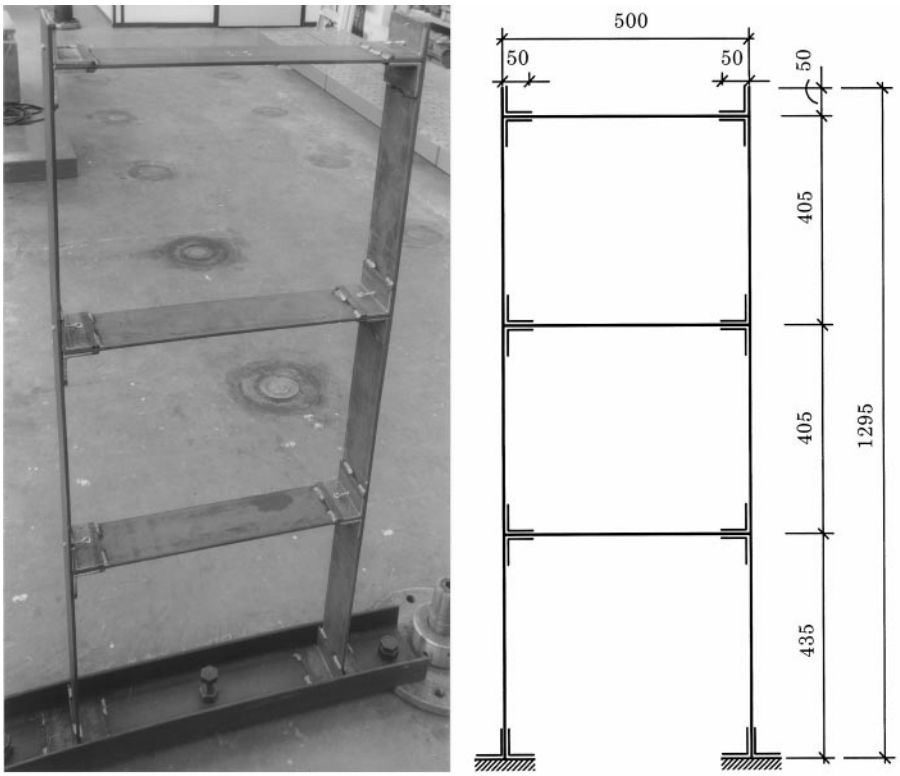

Figure 1. The experimental test frame and its dimensions, in mm.

TABLE 1

Modal parameters of the frame

Resonance frequency	Modal damping	Modal shape		
		First floor	Second floor	Third floor
$f_1 = 6{\cdot}25$ Hz	$\zeta_1 = 0{\cdot}15\%$	$v_1^T = \{$ 0·356	0·757	1·000$\}$
$f_2 = 20{\cdot}8$ Hz	$\zeta_2 = 0{\cdot}18\%$	$v_2^T = \{-1{\cdot}044$	$-0{\cdot}543$	1·000$\}$
$f_3 = 38{\cdot}3$ Hz	$\zeta_3 = 0{\cdot}12\%$	$v_3^T = \{$ 1·296	$-1{\cdot}479$	1·000$\}$

stripes with a 5×100 (mm^2) cross-section. The columns, floors and bottom U-profile are assembled by yielding these to corner steel elements with the same cross-section. These corner pieces enhance the stiffness against angular bending in the corners. The bottom U-profile is rigidly fixed to the floor of the laboratory.

The vibrations of the frame are considered to be restricted to be in its plane, due to its relatively low stiffness here. The three lowest natural modes have anti-symmetric mode shapes corresponding to an in- and out-of-phase movement of the three floors of the structure, as presented in Table 1. The next three natural frequencies 60, 81 and 97 Hz of the frame have symmetric mode shapes, characterized by the zero horizontal deflection of all floors. The next anti-symmetric modes have natural frequencies well over 100 Hz. A horizontal excitation of the first floor stimulates therefore practically only the three first anti-symmetric modes. Within an adequate low frequency band the frame can therefore be approximated by a three-degree-of-freedom system. The modal parameters presented in Table 1 are estimated by a standard modal analysis of the measured frequency responses of the frame. The details of the experimental set-up are presented in section 2.3.

2.2. THE COMBINED TUNED ABSORBER AND IMPACT DAMPER

The tuned absorber is built as a cantilevered mass attached to a floor of the frame by a set of two steel strips, allowing a practically horizontal movement of the absorber in the plane of the frame. Two collision plates can be fixed on the cantilevered mass at different positions, so that the distance between the two parallel plates can be varied with increments of 1 mm. The cantilevered mass and collision plates were built in aluminium to keep their mass low. A steel ball is used as the impact damper. The motion of the impact damper is kept free of external forces between impacts by suspending it into the gap between the two collision plates as a pendulum. The height of the pendulum is chosen to be considerably longer than the clearance to obtain a virtually pure translation of the ball.

2.3. THE EXPERIMENTAL SET-UP

The first floor of the test-frame is excited by a "white noise" force in a frequency band of width 6·25 Hz, centered on the fundamental frequency of the frame at 6·25 Hz. This is experimentally obtained by fixing a soft spring between the first floor and a shaker head, whose oscillations are controlled by the signal analyzer. The force level is experimentally set at an r.m.s. value of 1·5 N and corresponds to a one-sided power spectral density level of $S_0 = 0{\cdot}057$ N^{2}s/rad. The force and the acceleration of each floor and tuned absorber are measured, Fourier transformed and stored by the signal analyzer via the force transducer and accelerometers, respectively. The experimental set-up is shown in Figure 2.

3. THE NUMERICAL MODEL

3.1. THE PRIMARY STRUCTURE

The stiffness matrix K of the test frame can be accurately measured from a simple static experiment, which results in

$$K = \begin{Bmatrix} 193{\cdot}7 & -116{\cdot}9 & 24{\cdot}4 \\ -116{\cdot}9 & 175{\cdot}2 & -85{\cdot}1 \\ 24{\cdot}4 & -85{\cdot}1 & 65{\cdot}4 \end{Bmatrix} \times 10^3 \text{ N/m}. \tag{1}$$

The concentration of mass at each floor is not very high, so that a diagonal mass matrix evaluated from the mass distribution would be a rough approximation. Alternatively, the mass and damping matrices are fitted to the experimentally evaluated modal parameters, by solving the inverse eigenvalue problem, suggested in reference [9]. The excitation of the frame is restricted to the application of a force at the first floor of the frame. This procedure results in the following matrices:

$$M = \begin{Bmatrix} 6{\cdot}44 & 0{\cdot}66 & 0{\cdot}36 \\ 0{\cdot}03 & 5{\cdot}55 & -0{\cdot}37 \\ 0{\cdot}10 & 1{\cdot}06 & 5{\cdot}53 \end{Bmatrix} \text{kg}, \qquad F = \begin{Bmatrix} F(t) \\ 0 \\ 0 \end{Bmatrix} \text{N}, \tag{2, 3}$$

$$C = \begin{Bmatrix} 3{\cdot}04 & -0{\cdot}56 & -0{\cdot}29 \\ -0{\cdot}55 & 2{\cdot}18 & -1{\cdot}00 \\ -0{\cdot}40 & -0{\cdot}83 & 1{\cdot}51 \end{Bmatrix} \times 10^{-2} \text{ Ns/m}. \tag{4}$$

The resulting synthesized mass matrix is not perfectly diagonal, due to the relatively distributed mass of the frame. These matrices are not meant to describe a three-mass system in series (with spring and dampers connecting the masses), but should be considered as a synthetic system, built up to have the same response as the experimental structure. The numerical simulation of the model, based on the presented matrices M, C, K and F, shows, as expected, a good match with the experiments.

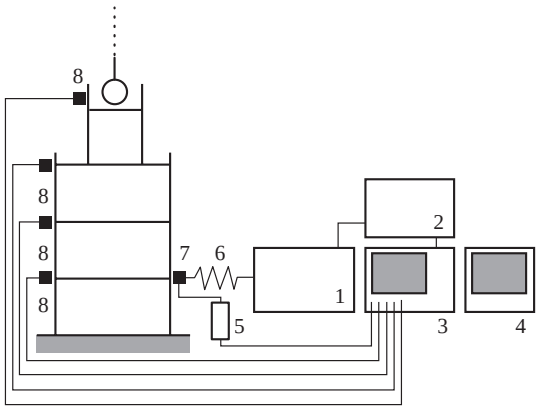

Figure 2. The experimental set-up: 1. "exciter body", Brüel & Kjaer 4802 with "big table head", Brüel & Kjaer 4848; 2. "Power amplifier" Bruel & Kjaer 2708; 3. "signal analyzer", Brüel & Kjaer 2035 with 2 × "4-channel input module", Brüel & Kjaer 3023; 4. personal computer; 5. "conditioning amplifier", Brüel & Kjaer 2626; 6. soft spring; 7. "force transducer", Brüel & Kjaer 8200; 8. "accelerometer", Brüel & Kjaer 4503.

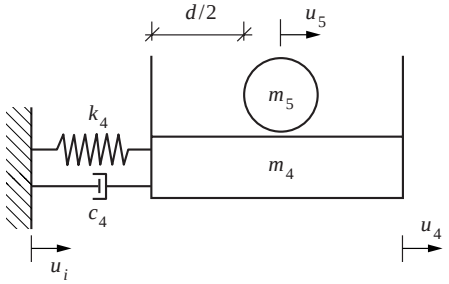

Figure 3. Model of the combined tuned absorber and impact damper.

3.2. THE COMBINED TUNED ABSORBER AND IMPACT DAMPER

Passive dynamic vibration absorbers are most effective, when attached where the vibration amplitude of the structure is the largest. The top floor of the frame should therefore be chosen to control the fundamental mode of the frame optimally.

The impact damper studied in this paper is considered to follow a translation trajectory without contact with the container between collisions. Impacts are considered instantaneous, as the duration of an impact is considerably shorter than the time between two consecutive collisions. These assumptions have generally been made in previous publications investigating this type of impact damper, because they lead to relatively simple experimental and numerical models [4–8].

The tuned absorber is a simple single-degree-of-freedom (1-d.o.f.) oscillator. The practically unavoidable damping of this system is considered to be viscous for convenience. The combined tuned absorber and impact damper is schematically presented in Figure 3, where u_i represents the displacement of the floor to which the system is attached. In this case, the third floor is considered.

In between impacts, the 5-d.o.f. combined system is described by the following set of linear differential equations:

$$\begin{Bmatrix} M_{11} & M_{12} & M_{13} & 0 & 0 \\ M_{21} & M_{22} & M_{23} & 0 & 0 \\ M_{31} & M_{32} & M_{33} & 0 & 0 \\ 0 & 0 & 0 & m_4 & 0 \\ 0 & 0 & 0 & 0 & m_5 \end{Bmatrix} \ddot{u} + \begin{Bmatrix} C_{11} & C_{12} & C_{13} & 0 & 0 \\ C_{12} & C_{22} & C_{23} & 0 & 0 \\ C_{13} & C_{32} & C_{33}+c_4 & -c_4 & 0 \\ 0 & 0 & -c_4 & c_4 & 0 \\ 0 & 0 & 0 & 0 & 0 \end{Bmatrix} \dot{u}$$

$$+ \begin{Bmatrix} K_{11} & K_{12} & K_{13} & 0 & 0 \\ K_{21} & K_{22} & K_{23} & 0 & 0 \\ K_{31} & K_{32} & K_{33}+k_4 & -k_4 & 0 \\ 0 & 0 & -k_4 & k_4 & 0 \\ 0 & 0 & 0 & 0 & 0 \end{Bmatrix} u = \begin{Bmatrix} F(t) \\ 0 \\ 0 \\ 0 \\ 0 \end{Bmatrix}. \tag{5}$$

Here m_4, c_4 and k_4 are the parameters of the tuned absorber, m_5 is the mass of the impact damper and M_{ij}, C_{ij} and K_{ij} refer to the system matrices in equations (1), (2) and (4).

The collisions are idealized as discontinuous processes governed by the conservation of momentum, and the definition of the coefficient of restitution. The velocities of m_4 and m_5 just before and immediately after a collision are thereby related by the equations

$$\dot{u}_4^+ = \frac{(1-\eta e)}{(1+\eta)}\dot{u}_4^- + \frac{\eta(1+e)}{(1+\eta)}\dot{u}_5^-, \qquad \dot{u}_5^+ = \frac{(1+e)}{(1+\eta)}\dot{u}_4^- + \frac{(\eta-e)}{(1+\eta)}\dot{u}_5^-, \tag{6}$$

where η is the mass ratio m_5/m_4 and the restitution coefficient e is defined by

$$e = -(\dot{u}_5^+ - \dot{u}_4^+)/(\dot{u}_5^- - \dot{u}_4^-). \tag{7}$$

The superscripts $-$ and $+$ refer to states just before and immediately after a collision, respectively.

As the system with the absorber is linear between impacts, its behavior can be simulated by a numerical integration until contact between m_4 and m_5 is found. The fourth order Runge–Kutta integration method, with time steps smaller than 1/40 of the lowest excitation period, is chosen. An impact is assumed when the relative distance between m_4 and m_5 is found to be less than 10^{-6} of the clearance d. The bisection procedure is used to locate an impact. At impact, the velocities of m_4 and m_5 are changed according to equations (6), leaving all other parameters unchanged. The integration is then resumed with new initial conditions until another impact is detected.

3.3. THE RANDOM EXCITATION

Numerically, the "white noise" excitation is simulated by using the trigonometric polynomial [10]

$$P(t) = \sqrt{2S_0 \frac{2\omega}{2n+1}} \left[\frac{1}{2} \sin U_0 + \sum_{k=1}^{n} \sin \left(k \frac{\omega}{n} t + U_k \right) \right], \tag{8}$$

where ω is the maximal cyclic frequency of the excitation band set at $2\pi \times 12{\cdot}5$ Hz, n is the number of frequencies in the sum, set here at 800 to match the signal from the analyzer used in the experiments, S_0 is the one-sided power spectral density $S_0 = 0{\cdot}057$ N^{2}s/rad, corresponding to the experimental force level set at an r.m.s. value of 1·5 N, and U_0, $U_1 \ldots U_n$ are mutually independent random variables, that are uniformly distributed on the interval $[0,2\pi]$.

The experimental "white noise" excitation in a frequency band of width 6·25 Hz, centered on the fundamental frequency of the frame at 6·25 Hz, can be simulated by including only the elements of the sum in equation (8) corresponding to $200 < k \leqslant 600$. This limitation of the "white noise" excitation to a frequency band around the resonance frequency considerably reduces the computation time. As the fundamental mode considered is low damped and well separated from the others ($\omega_2 \geqslant 3\omega_1$), it can be considered as a single one in the case of the linear tuned mass damper [3, 11]. By exciting only within a frequency band around the fundamental frequency, the eventual influence of higher modes on the non-linear combined absorber is practically eliminated. In this paper, therefore, only the control of a single natural frequency is considered. This case is more general, as the effect of higher modes is specific to the structure considered. In reference [12] the response of the experimental frame with optimal combined absorber around its fundamental frequency is found to be unaffected by its higher modes.

4. EXPERIMENTAL RESULTS AND NUMERICAL SIMULATIONS

The experimental and the simulated response of the third floor of the frame without the absorber has an r.m.s. displacement of $\sigma_{x0} \approx 7{\cdot}7 \times 10^{-4}$ m. This value is chosen as the reference for the cases studied.

By measuring both the acceleration of the tuned mass and that of its attachment point on the third floor, it is simple to analyze the relative oscillations of the tuned absorber as that of a simple 1-d.o.f. system subjected to a ground motion. A standard modal analysis of the frequency response of the absorber estimates the natural frequency and damping

ratio of the tuned absorber. The stiffness k_4 of the springs is calculated from this identified natural frequency and the weighted mass of the cantilevered absorber and part of the steel strips. The parameters are found at $m_4 = 0{\cdot}250$ kg, $c_4 = 0{\cdot}08$ Ns/m and $k_4 = 372$ N/m. This linear model of the tuned absorber is found to be reasonably accurate.

The restitution coefficient is evaluated experimentally from the measured relative rebound of a pendulum after impact with a fixed collision plate. For relative velocities over 2 m/s before impact, the coefficient of restitution for the impact of a steel ball on an aluminum plate is found to be nearly constant around 0·3. The computational calculations show that the velocities before impact are mostly concentrated under 0·2 m/s, for which the restitution coefficient for the impact of a steel ball on an aluminum plate is evaluated to be approximately 0·7. The steel ball chosen as the impact damper has a mass of $66{\cdot}7 \times 10^{-3}$ kg corresponding to a mass ratio to the tuned absorber, $\eta = m_5/m_4 = 27\%$.

The frequency response of the experimental system is collected, Fourier transformed and averaged by the signal analyzer. The numerically simulated responses of the system were also processed by the same signal analyzer, as if these were measured experimental data. Figure 4 presents both the numerical and the experimental frequency responses for selected non-dimensionalized clearances d/σ_{x0}, where d and σ_{x0} are, respectively, the clearance and the r.m.s. displacement of the primary system without absorber.

The system with tuned absorber alone in Figure 4(h), corresponds to the case of infinite clearance ($d/\sigma_x \to \infty$), where collisions never occur. Reducing the clearance increases the number of collisions and the effectiveness of the combined absorber. This results in the reduction of the two peaks, as observed when comparing Figure 4(h) with Figures 4(g), 4(f) and 4(e). A further decrease of the clearance can result in such a large reduction of the oscillations of the tuned absorber, that the oscillations of the primary structure appear (see Figue 4(d)). Smaller clearances increase the number of impacts, so that several impacts can be observed on the same side before collision with the opposite side. The control effectiveness from the momentum transfer between impact damper and the tuned absorber is thereby deteriorated (see Figure 4(c)). A further reduction of the clearance leads to the carrying of the impact damper by the tuned absorber for short periods (see Figure 4(b)), converging towards the added mass situation for zero clearance presented in Figure 4(a). This last case corresponds to a system with an off-tuned tuned absorber.

The experimental and computational frequency responses presented in Figure 4 are in good concordance. The computational model seems to be quite accurate, even in the vicinity of the optimal clearance (see Figure 4(d)), where the shape of the frequency response undergoes a radical change, which is sensitive to any parameter inaccuracy.

The r.m.s. displacements of these responses are calculated and non-dimensionalized by the r.m.s. displacement of the primary system without absorber σ_{x0}. These relative r.m.s. displacements are presented in Figure 5 for different non-dimensional clearances. The concordance between the numerical and experimental results is satisfactory, considering the difficulties in defining a ''constant'' coefficient of restitution at low impact velocities.

In Figure 5, an ordinate of 1 would correspond to the case where the r.m.s. displacement of the frame is unaffected by the introduction of the absorber. A reduction of the r.m.s. displacement of the frame of about 70% can be observed over a wide range of clearances. The introduction of the impact damper clearly enhances the effectiveness of the lightly damped absorber for clearances over $d/\sigma_{x0} = 5$. The flatness of the experimental and numerical curves in Figure 5 shows an advantageous robustness of the combined absorber against changes in the non-dimensional clearance.

The numerical model of the tuned absorber and that of the impact damper seems to be accurate, when comparing the experimental and numerical results obtained here for a relatively high value of the coefficient of restitution. A similar experimental investigation

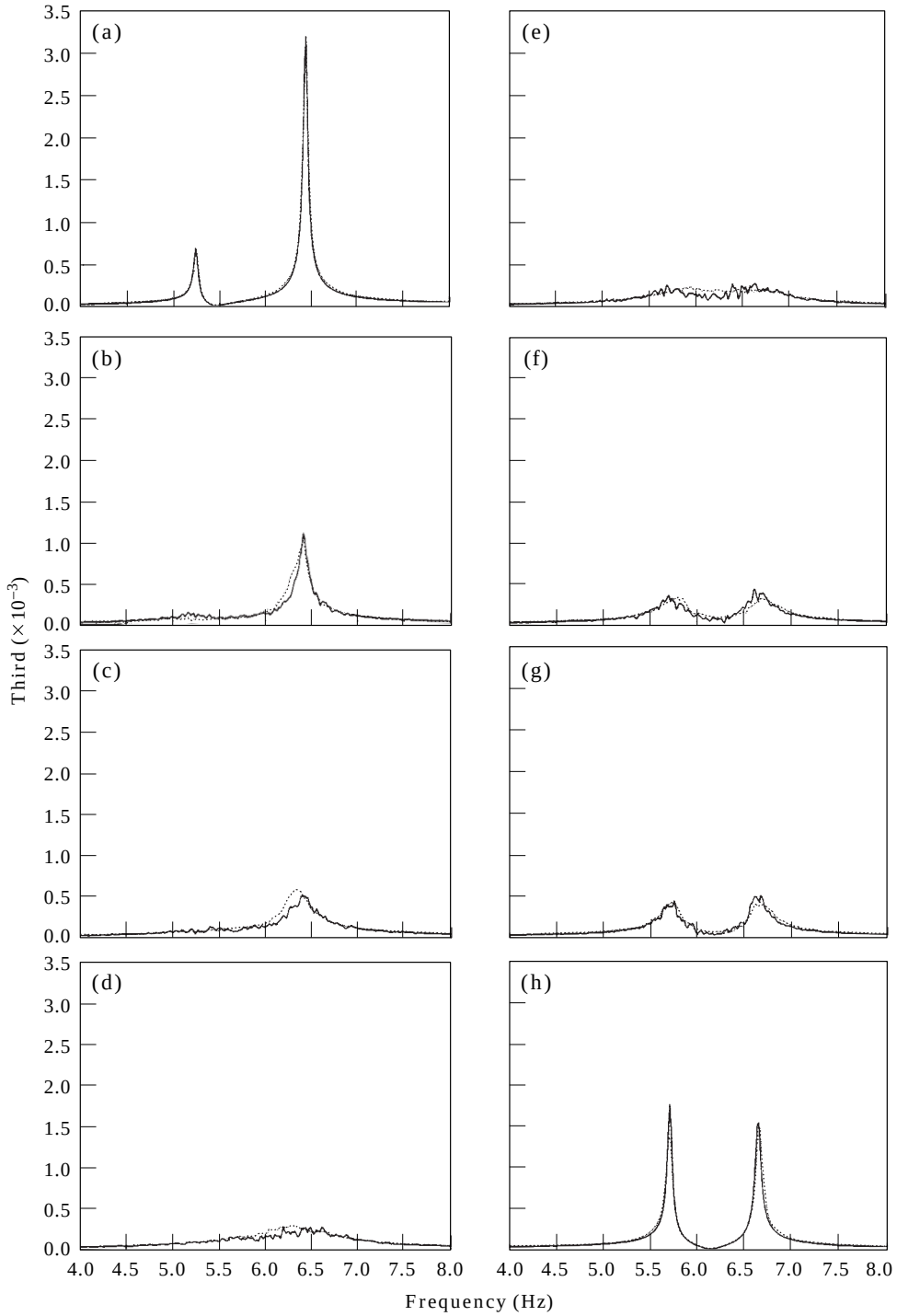

Figure 4. The numerical (——) and experimental (. . .) frequency responses of the displacement of the third floor per unit force applied on the first floor of the frame with combined absorber on the third floor for chosen clearances. d/σ_{x0}: (a) 0, (b) 4·7, (c) 7·3, (d) 12·5, (e) 17·7, (f) 24·2, (g) 43·6, (h) ∞.

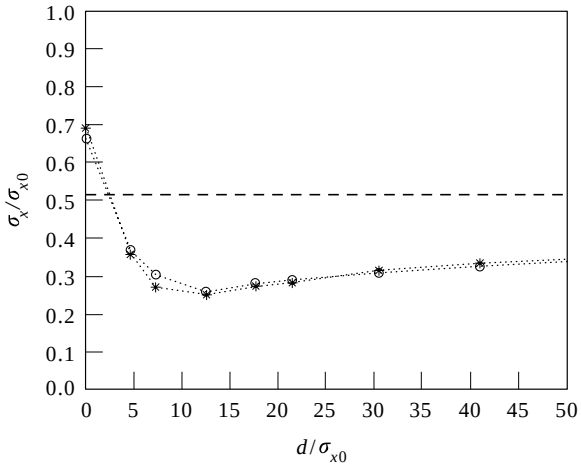

Figure 5. Numerical (*) and experimental (○) relative r.m.s. displacement for chosen clearances. The tuned absorber without impact damper ($d/\sigma_{x0} \to \infty$) is presented by (——) for comparison.

with a lower coefficient of restitution would be necessary to validate the model in general, as plastic deformation is expected in the case of low coefficients of restitution. Materials such as different metals, Plexiglas and neoprene rubber lined plates have been considered for the collision plates in order to have a wide range of restitution coefficients, but this was only possible for relative velocities over 2 m/s.

The lowest coefficient of about 0·15 was attained for steel-lead collisions, but corresponded to approximately 0·75 for relative velocities under 0·2 m/s. Low coefficients of restitution can be difficult to achieve in practice, if the relative velocities at impact are low. If one considers a specific pattern of the impacts around resonant oscillations, then these relative velocities seem to increase with an increasing resonance frequency and with an increasing oscillation amplitude. In the case of controlling civil engineering structures, which have typically natural frequencies under 1 Hz, low impact velocities are expected and high restitution coefficients will have to be considered.

5. NUMERICAL OPTIMIZATION AND PARAMETER SENSITIVITY ANALYSIS

The numerical model describes the absorber by the impact damper parameters m_5 and e and the tuned absorber parameters m_4, c_4 and k_4. The elaborated computational model is used to optimize the combined absorber and investigate its sensitivity to a variation of its parameters away from optimum.

In order to evaluate the effect of the introduction of an impact damper as the only damping mechanism of the combined absorber, the viscous damping of the tuned absorber is disregarded in the following numerical models. The effect of damping in the absorber will be investigated at the closure of this section.

5.1. THE IMPACT DAMPER PARAMETERS

The impact parameters regarded for optimization are the clearance d, which is non-dimensionalized with the r.m.s. displacement of the third floor of the frame without absorber as d/σ_{x0}, the mass ratio η between the impact damper and the tuned absorber, and the restitution coefficient e.

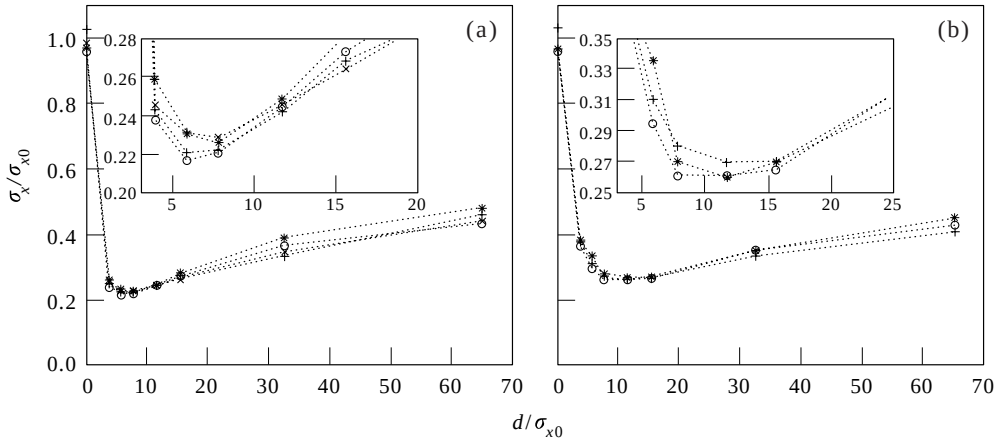

Figure 6. Relative r.m.s. displacement for chosen clearances and mass ratio η for a restitution coefficient of (a) 0·3 and (b) 0·7. η values: *, 0·13; ○, 0·25; +, 0·50; ×, 0·75.

The general variation of the effectiveness of the combined absorber with the clearance is similar, for any parameter choice presented in Figures 6 and 7 as well as the special experimental case in Figure 5. The introduction of the combined system can reduce the r.m.s. displacement of the third floor of the frame by nearly 80% at clearances $d/\sigma_{x0} \approx 6$, if the restitution coefficient can be set as low as 0·3.

The results presented in Figure 6 show a relatively low sensitivity to a variation of the mass ratio around the optimal $\eta = 0{\cdot}25$, for restitution coefficients of both 0·3 and 0·7. This trend was also observed experimentally by varying the size and thereby the mass of the suspended impact damper. A much lower mass ratio would, however, reduce the momentum transfer between the impact damper and tuned absorber, reducing thereby the effectiveness of the combined absorber. A mass ratio higher than optimum, but still under 1, would increase this impulse transfer, reducing the relative oscillations of the tuned absorber to a minimum. This would result in unwanted excessive vibrations at the

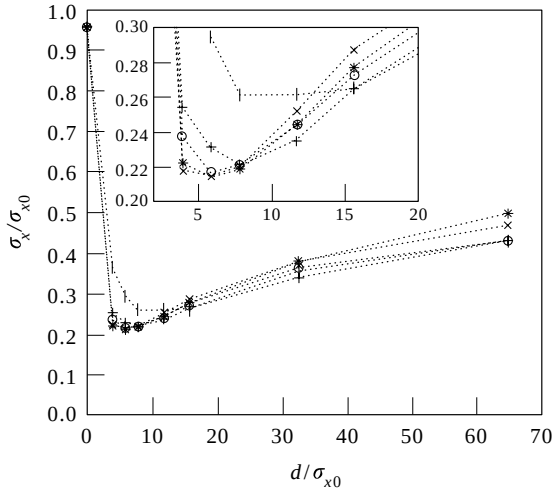

Figure 7. Relative r.m.s. displacement for chosen clearances and restitution coefficients but for $\eta = 0{\cdot}25$. e values: ×, 0·1; *, 0·2; ○, 0·3; +, 0·4, l, 0·7.

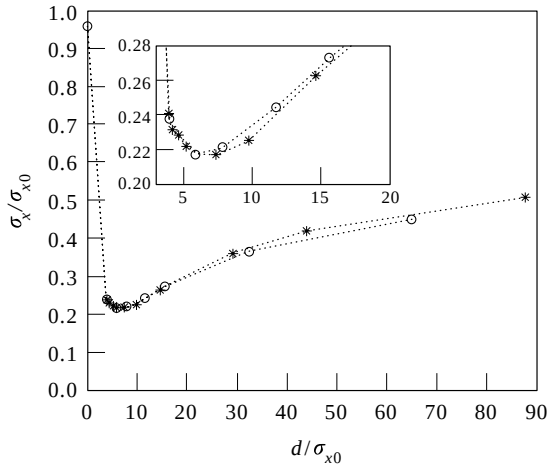

Figure 8. Relative r.m.s. displacement for different non-dimensional clearances obtained by changing (*) the level of excitation for $d = 4{\cdot}5$ mm or (○) the clearance d for an r.m.s. amplitude of the excitation force of 1·5 N ($\eta = 0{\cdot}25$, $e = 0{\cdot}3$).

resonance of the main structure with added mass, corresponding to the immobilized tuned absorber.

Figure 7 shows that a low restitution coefficient e between 0·1 and 0·3 has nearly the same optimal effectiveness for clearances $d/\sigma_{x0} \approx 6$. A higher restitution coefficient increases the velocity of the impact damper and reduces the energy dissipation at each collision in general. To maintain a similar optimal impact pattern, this results in a shift of the optimal clearance to higher values as well as a reduction of the effectiveness of the combined absorber. Very low restitution coefficients are practically unattainable and problematic, because of material deformation. A restitution coefficient of $e = 0{\cdot}3$ is therefore the most suitable choice as the optimum.

The numerical case studies were conducted for a constant excitation level corresponding to a r.m.s. force of $\sigma_p = 1{\cdot}5$ N resulting in a r.m.s. displacement of the third floor of the frame of $\sigma_{x0} = 770 \times 10^{-6}$ m. The optimal parameters are found to be $\eta = 0{\cdot}25$, $e = 0{\cdot}3$ and $d \approx 6 \times 770 \times 10^{-6}$ m $\approx 4{\cdot}5$ mm. A variation of the excitation level will proportionally change the response σ_{x0} of the uncontrolled linear frame and thereby the non-dimensionalized clearance d/σ_{x0}, for a constant d. The relative r.m.s. response of the third floor of the frame with combined absorber for different excitation levels, is presented in Figure 8. The relative r.m.s. response of the third floor corresponding to a variation of the clearance d for a constant load level from Figures 6 and 7 is also presented in Figure 8 for comparison. Both curves are in good concordance, which confirms that the quotient d/σ_{x0} is a non-dimensional parameter for the combined absorber.

5.2. THE TUNED ABSORBER PARAMETERS

The optimal parameters of the conventional tuned mass damper TMD are presented and evaluated for the considered primary structure, in order to compare it to the optimal combined absorber.

5.2.1. *The optimal tuned mass damper*

The natural frequency and viscous damping ratio are the main optimization parameters of a TMD. Analytical expressions for these optimal parameters are presented in references

TABLE 2

Optimal parameters of the TMD, where v is the mass ratio between the tuned absorber and the main 1-d.o.f. system

Optimal tuning frequency	Optimal damping ratio
$\gamma_m^{opt} = \sqrt{\frac{1 + 0{\cdot}5v}{(1+v)^2}}$	$\zeta_2^{opt} = \sqrt{\frac{v(1 + 0{\cdot}75v)}{4(1 + 0{\cdot}5v)(1+v)}}$

[3] and [11] for a TMD attached to an undamped 1-d.o.f. system under white noise excitation.

The formulas in Table 2 are used to evaluate the optimal TMD parameters for the experimental frame, by regarding its oscillations around the fundamental frequency as that of a simple 1-d.o.f. system. This is acceptable because of the minimal influence of the higher modes around the fundamental frequency of the frame and the low damping of this fundamental mode [11]. This 1-d.o.f. system is based on the modal mass of the frame at the attachment point of the absorber.

Based on the mass matrix M given in equation (2), and the eigenvectors given in Table 1, the modal mass of the frame at the point of attachment of the absorber is evaluated as [3, 11]

$$m_{1,eff} = (1/v_1^3)^2 \{v_1\}^T [M] \{v_1\} = 10{\cdot}3 \text{ kg}, \tag{9}$$

where v_1^3 is the value of the fundamental eigenvector corresponding to the point of attachment of the absorber (third floor).

5.2.2. *The viscous tuned mass parameters*

The essential parameter for the performance of a tuned absorber is its frequency tuning to the primary structure. The natural frequencies f_{abs} of the tuned absorbers are varied by choosing different values for the stiffness k_4. The tuning frequencies of both optimal TMD's presented in Table 3 are varied in the same way and the corresponding r.m.s. displacement responses of the different absorbers are presented in Figure 9 for comparison. Figure 9 shows that the optimal tuning frequency of a TMD is lower than that for the combined absorber. The reason for a higher optimal frequency of the tuned absorbers within the combined absorbers is to compensate the added mass effect of the impact damper. In this case, the optimal tuning frequencies of these tuned absorbers are found to be both around 6·6 Hz. On the other hand, the optimal effectiveness of the combined absorber with a high restitution coefficient (0·7) is about 5% less than that corresponding to one with the lower restitution coefficient (0·3).

TABLE 3

Optimal TMD parameters for two different mass ratios

Absorber mass	Mass ratio v	Optimal frequency	Stiffness k_4	Optimal damping	Damping coefficient c_4
$m_{abs} = m_4$ $= 0{\cdot}250$ kg	2·4%	6·14 Hz	372 N/m	7·7%	1·5 Ns/m
$m_{abs} = (1 + \eta_{opt})m_4$ $= 0{\cdot}3125$ kg	3·0%	6·11 Hz	461 N/m	8·6%	2·1 Ns/m

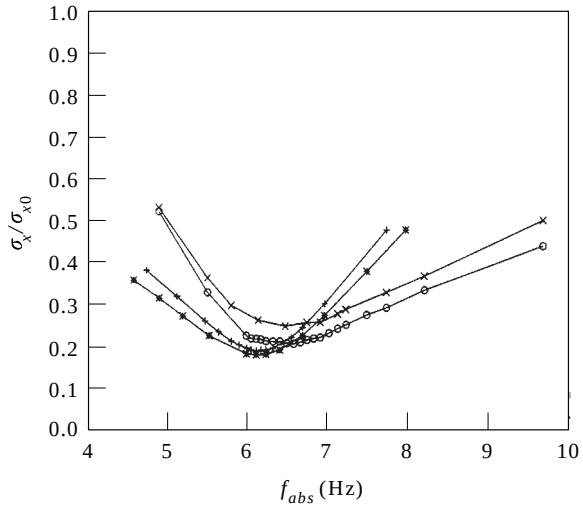

Figure 9. Relative r.m.s. displacement for different natural frequencies of the tuned absorber within the combined absorber ($m_4 = 0{\cdot}25$ kg, $m_5 = \eta_{opt}\ m_4$) with a restitution coefficient (○) $e = 0{\cdot}3$ and (×) $e = 0{\cdot}7$ and the optimal tuned mass dampers with a mass of (+) $m_{abs} = m_4$ and (*) $m_{abs} = m_4\ (1 + \eta_{opt})$.

The introduction of an impact damper into an undamped tuned mass m_4 has practically the same effectiveness (80% reduction at optimum), as the introduction of a viscous damping to the conventional tuned absorber. Unfortunately, the introduction of the impact damper into the tuned absorber adds mass to the absorber. The performance of the combined absorber should therefore be compared to that of the optimal TMD with a mass corresponding to the sum of the mass of the tuned mass and impact damper. In this case, the effectiveness of the conventional TMD at optimum is enhanced to a 82% reduction. On the other hand, the combined absorbers are more robust to variations of the frequency tuning.

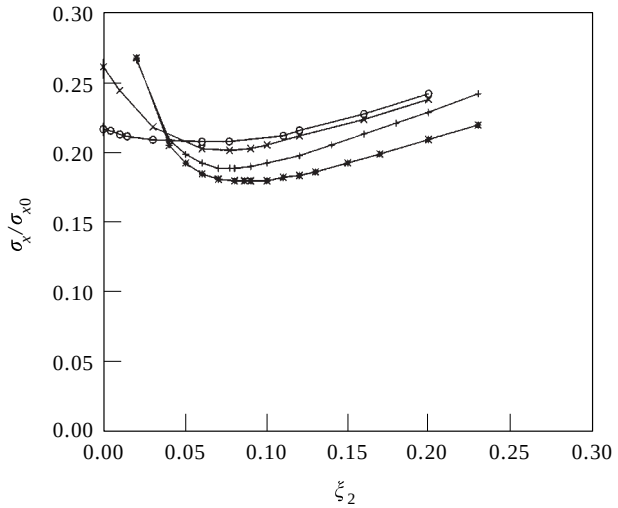

Figure 10. Relative r.m.s. displacement for different damping ratios of the tuned absorber within the combined absorber ($m_4 = 0{\cdot}25$ kg, $m_5 = \eta_{opt}\ m_4$) with a restitution coefficient (○) $e = 0{\cdot}3$ and (×) $e = 0{\cdot}7$ and the optimal tuned mass dampers with a mass of (+) $m_{abs} = m_4$ and (*) $m_{abs} = m_4\ (1 + \eta_{opt})$.

The effect of the presence of the viscous damping ζ_2 in the optimal tuned absorbers in both the conventional TMD and the combined absorbers is presented in Figure 10. In the case of the conventional TMD, the presence of damping is critical to its effectiveness. An unexpected loss of pressure in a hydraulic damper often used as viscous elements in TMDs is unacceptable. On the other hand, the unavoidable presence of a light damping in the tuned absorber within the optimal combined absorber with a high restitution coefficient ($e = 0{\cdot}7$) enhances rapidly its effectiveness. It is also interesting to notice that the introduction of the impact damper would reduce the effectiveness of the optimal TMD.

6. CONCLUSION

A combined tuned absorber and impact damper has been investigated by numerical simulations and experimental observations. The optimal mass ratio between the impact damper and tuned absorber was found to be 25%, with a low sensitivity to variations of this mass ratio. The restitution coefficient seems to be optimal around 0·3, but the effectiveness and sensitivity of the combined absorber for higher and more practical restitution coefficients around 0·7 are satisfactory. The clearance is found to be directly proportional to the excitation level, if the primary system can be considered linear-elastic. The tuned absorber within the combined absorber should be tuned to a frequency slightly higher than the optimal tuning frequency of the corresponding TMD. The combined absorber is found to be more robust than the corresponding TMD to variations of the tuning of the tuned absorber.

Such a combined absorber optimized for a given critical excitation level is almost as effective as that of the corresponding TMD. A lower excitation amplitude would not affect the performance of the TMD, but would somewhat reduce the effectiveness of the combined absorber to a still very satisfactory level.

The investigated combined absorber seems to be a cheap alternative to the Tuned Mass Damper, although its practical use may be limited by the geometric requirement to suspend the impact damper in the tuned absorber. A further study of a combined absorber based on an impact damper rolling directly in its cavity is being made, and is promising.

ACKNOWLEDGMENT

The Danish Research Councils (STVF) are gratefully acknowledged for their financial support.

REFERENCES

1. J. P. Den Hartog 1956 *Mechanical Vibrations*. New York: McGraw-Hill.
2. H. B. Hunt 1979 *Dynamic Vibration Absorbers*. Mechanical Engineering Publications Ltd.
3. B. G. Korenev and L. M. Reznikov 1993 *Dynamic Vibration Absorbers*. New York: John Wiley.
4. S. F. Masri and A. M. Ibrahim 1973 *Journal of the Acoustical Society of America* **53**, 200–211. Response of the impact damper to stationary random excitation.
5. C. N. Bapat and S. Sankar 1985 *Journal of Sound and Vibration* **99**, 85–94. Single unit damper in free and forced vibration.
6. S. E. Semercigil, N. Popplewell and R. Tyc 1988 *Journal of Sound and Vibration* **121**, 178–184. Impact damping of random vibrations.
7. S. E. Semercigil, D. Lammers and Z. Ying 1992 *Journal of Sound and Vibration* **156**, 445–459. A new tuned vibration absorber for wide band excitations.
8. Z. Ying and S. E. Semercigil 1991 *Journal of Sound and Vibration* **150**, 520–530. Response of a new tuned vibration absorber to an earthquake-like random excitation.

9. L. STAREK and D. J. INMAN 1991 *Proceedings of the 9th International Modal Analysis Conference IMAC* **1**, 352–355. Solution of the model correction problem via inverse methods.
10. O. DITLEVSEN and L. BÒGNAR 1993 *Probabilistic Engineering Mechanics* **8**, 209–231. Plastic displacement distributions of the Gaussian white noise excited elastoplastic oscillator.
11. G. B. WARBURTON 1982 *Earthquake Engineering and Structural Dynamics* **10**, 381–401. Optimum absorber parameters for various combinations of response and excitation parameters.
12. F. S. COLLETTE 1997 *Ph.D. Thesis*, *Department of Structural Engineering and Materials*, *Technical University of Denmark*. A combined tuned absorber and impact damper under random excitation.